Available online at www.sciencedirect.com

ScienceDirect

Mendeleev Commun., 2021, **31**, 154–156

Mendeleev Communications

Photochemical transformations of *exo*-2,3-norbornene oxide radical cations in the CF_3CCl_3 matrix at 77 K

Daria A. Pomogailo,*[a,b] Ivan D. Sorokin,[a] Oleg I. Gromov,[a] Vladimir I. Pergushov[a] and Mikhail Ya. Melnikov[a]

[a] *Department of Chemistry, M. V. Lomonosov Moscow State University, 119991 Moscow, Russian Federation. E-mail: texafirin@ya.ru*

[b] *Russian Institute for Scientific and Technical Information, Russian Academy of Sciences, 125190 Moscow, Russian Federation*

DOI: 10.1016/j.mencom.2021.03.003

The structure and nature of the underlying photochemical transformations of radical cations formed upon irradiation of *exo*-2,3-norbornene oxide solutions in a CF_3CCl_3 matrix at 77 K have been established using electron paramagnetic resonance and UV-visible absorption spectroscopy as well as quantum chemical calculations. For photochemical reactions proceeding in this system, a mechanism has been proposed, which consists in the transformation of the initially formed ring-open radical cation into a ring-closed C-centered radical cation, followed by photoelimination of H_2.

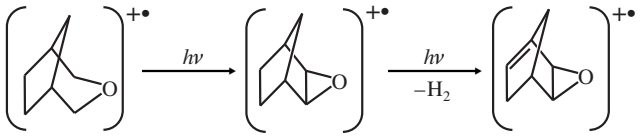

Keywords: *exo*-2,3-norbornene oxide, radical cations, matrix stabilization, freon matrices, photochemistry, EPR spectroscopy, electronic absorption spectroscopy, quantum chemical calculations.

Studies of radical ion intermediates, including electronically excited radical ions, and their reactivity are of great interest due to the role that these species play in the chemistry of processes triggered in various substances under extreme conditions, from astrochemistry to reactions in living systems upon ionizing irradiation.[1–3] Earlier, when investigating transformations in a series of radical cations (RCs) produced from methyl-substituted oxiranes stabilized in Freons at 77 K,[4,5] it was found that the RCs under consideration exist either in a ring-open form, afforded by C–C bond cleavage in the oxirane ring, or in a ring-closed form. It was also shown that some oxiranes are characterized by reversible mutual phototransformations between these RC forms.

Under similar conditions, the RCs of compounds that include both an oxirane ring and an alicycle in their structures (cyclohexene oxide, cyclopentene oxide) are stabilized in forms characterized by an elongated C–C bond in their oxirane fragment.[6,7] Unlike the RCs of methyloxiranes, the main mechanism of phototransformation of these RCs involves deprotonation, resulting in the formation of C-centered radicals as the end products of the reaction.

Since different types of RCs derived from substituted oxiranes behave differently under the action of light, the problem arises of establishing a relationship between the structure of the precursor and the nature of RCs stabilized under indirect ionization, together with the problem of predicting the mechanisms of subsequent photochemical transformations based on structural knowledge. To further this cause, the structure and transformations of the RC derived from *exo*-2,3-norbornene oxide (ENBO) were investigated. This species is very interesting, since its precursor molecule includes structural motifs of cyclohexene oxide and cyclopentene oxide, and these are two oxirane-derived RCs whose phototransformations have already been investigated.[6,7] No data on phototransformation of RCs with two or more conjugated alicycles have been documented up to now. It was interesting to find out whether the relationship between structure and reactivity is vital for predicting the behavior of RCs under the action of light. Also, it was curious to use this type of RC to prove the predictive capabilities of quantum chemical calculations for such rather complex structures.

ENBO RCs were obtained by irradiation of frozen ENBO/CF_3CCl_3[†] solutions (~0.3 mol%) at 77 K. The method of Freon synthesis, sample preparation procedures, irradiation techniques, detection methodology related to electron paramagnetic resonance (EPR) and UV-visible absorption (UV-VIS) spectra, as well as the photochemical experiment procedure were described in detail in an earlier work.[4] Quantum chemical calculations were mainly performed by the unrestricted density functional theory (DFT) method using the ORCA 4.1.1 software package.[8] The B3LYP and B2PLYP functionals,[9] together with the full-electron def2-TZVP basis set,[10] were used to calculate the geometry of the potential energy surface (PES) minima. The geometry at the minima was additionally checked for the presence of imaginary vibration frequencies. The parameters of the spin Hamiltonian were calculated using the B3LYP functional together with the full-electron N07D basis set.[11] An effect of the solvent was taken into account using the COSMO model.[12] The DFT calculations for the ENBO RC have shown that there are two minima on the corresponding PES, which can be represented

[†] Freon CF_3CCl_3 (>99% based on NMR data) prepared from $CF_2ClCFCl_2$ (~99%, Aldrich) was used as the matrix. The ENBO substrate (~97%, Aldrich) was used without additional purification.

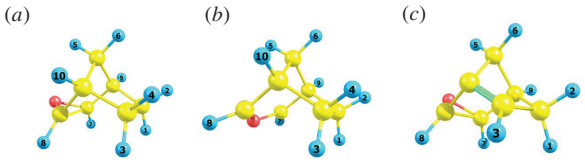

1 **2** **3**

Figure 1 Calculated (DFT/B2PLYP/def2-TZVP) structures of the ENBO-derived RCs (*a*) **1** and (*b*) **2**, which can form in irradiated ENBO/CF_3CCl_3 solutions, as well as (*c*) the structure of 3-oxatricyclo[3.2.1.$0^{2,4}$]oct-5-ene RC (**3**). The distances between two carbon atoms in the oxirane ring are given.

by two structures **1** and **2** [Figures 1(*a*),(*b*)], in which the distances between the carbon atoms in the oxirane rings are ~1.78 and ~2.32 Å, respectively. Their relative full energies are predicted to be 114.9 and 0 kJ mol^{-1}, respectively, which is in good agreement with reported data.[5] These data suggest that ring-open RC forms of substituted oxiranes, which have a cleaved C–C bond in the oxirane ring, are energetically preferred. The calculated magnetic resonance parameters given in Table 1 show that the sets of hyperfine coupling (hfc) constants corresponding to structures **1** and **2** are characteristically different, which should manifest itself in different experimental EPR spectra for these species.

The EPR spectrum measured upon irradiation of frozen ENBO/CF_3CCl_3 solutions can be interpreted as a multiplet signal [Figure 2(*a*)].‡ However, upon warming the irradiated samples from 77 to 130 K, changes in the EPR spectrum are observed [Figure 2(*a*), inset]; upon subsequent cooling to 77 K, the original signal is practically restored. For the radiolysis product at 130 K, the central region of the EPR spectrum [Figure 2(*a*), inset, curve *1*] can be adequately fitted [Figure 2(*a*), inset, curve *2*] using the magnetic resonance parameters (see Table 1) that are close to those calculated for form **2** [see Figure 1(*b*)], excluding those calculated for form **1**.

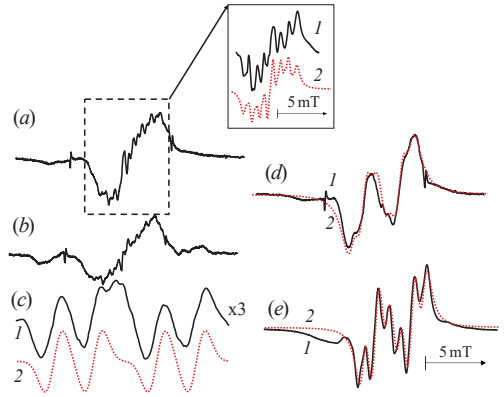

Figure 2 EPR spectra recorded (*a*) at 77 K immediately after irradiation of frozen ENBO/CF_3CCl_3 solutions (inset: the central part of the spectrum recorded at 130 K) and its simulation (*b*) during subsequent photolysis at 77 K (λ > 400 nm) at the highest detected content of side components. (*c*) Difference EPR spectrum of paramagnetic species forming and perishing during the photolysis of ENBO RC at 77 K. EPR spectra of the final photolysis product recorded at (*d*) 77 and (*e*) 130 K. (*1*) Experimental spectra, (*2*) simulation results (for fitting parameters see text and Table 1). All EPR spectra recorded in this work have a Lorentzian line shape with varying line widths. The line width of the simulated curve *2* amounts to (*a*, inset) 0.45, (*c*) 3.0, (*d*) 1.0 and (*e*) 0.75 mT.

‡ Hereinafter, the experimental EPR spectra are given and attested after their photobleaching, in which some Freon centers are removed by visible and near-IR light, and the residual signals of Freon radicals are removed by simply subtracting the corresponding experimental EPR spectra.

Table 1 DFT/B3LYP/N07D quantum chemical calculation results for isotropic hfc constants *a* to hydrogen nuclei and *g*-tensor components of the ENBO-derived RCs.

RC	*a*/mT									
	H^1	H^2	H^3	H^4	H^5	H^6	H^7	H^8	H^9	H^{10}
1	1.02	1.02	2.45	2.45	<0.1	0.15	<0.1	0.15	0.19	<0.1
	g_{xx} = 2.0027, g_{yy} = 2.0057, g_{zz} = 2.0050									
2[a]	1.70 (1.96)	1.70 (1.47)	<0.1	<0.1	<0.1	0.86 (0.83)	<0.1	0.86 (0.70)	0.23 (0.35)	0.12
	g_{xx} = 2.0018, g_{yy} = 2.0020, g_{zz} = 2.0023									

[a] The corresponding fitting parameters of EPR spectrum are given in parentheses.

Simultaneously with the formation of paramagnetic centers upon irradiation of ENBO/CF_3CCl_3 solutions at 77 K, an absorption band appears in the UV-VIS spectra with a maximum at ~550 nm [Figure 3(*a*)]. It is assumed that both the absorption band with a maximum at ~550 nm and the EPR spectrum obtained upon irradiation at 77 K [see Figure 2(*a*)] can be attributed to ENBO RCs in form **2**. Subsequent exposure to light with $\lambda \geqslant 400$ nm leads to the disappearance of the absorption band, and the EPR spectrum of RC **2** is simultaneously transformed into the spectrum of different paramagnetic species.

Step-by-step changes in the UV-VIS spectra during photolysis are shown in Figure 3(*a*). Notably, a small redshift is observed along with the decrease in absorbance at the maximum. This effect becomes evident in the difference spectra measured at different stages of the photolysis process and normalized by absorbance at the corresponding absorption maxima [Figure 3(*b*)]. The species responsible for the observed spectral shift are formed and completely consumed during the photolysis process. Their formation and depletion during photolysis are associated with the observed changes in the EPR spectra (see Figure 2), where at the intermediate stages of photolysis, along with a decrease in the concentration of RC **2**, new components appear in the low-field and high-field regions of the spectrum. At the photolysis stage, which was estimated to correspond to the highest concentration of the described species, their EPR spectra could be identified [Figure 2(*b*)]. The full spectrum obtained by subtracting the EPR spectrum of the radiolysis product from the EPR spectrum corresponding to the highest content of the low-field and high-field components is given in Figure 2(*c*) (curve *1*), where its fitting is also presented (curve *2*). This difference EPR spectrum is a four-line signal with splittings of ~3.3 and ~8.6 mT. Analogous EPR spectra with the values of the hfc constants marginally differing from the splittings measured in this work were previously[13,14] observed for RCs of alkyl-substituted cyclohexanes stabilized in Freons at 77 K, while their point symmetry was as low as C_s.

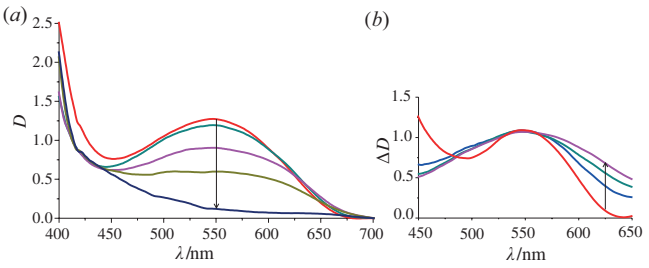

Figure 3 (*a*) Changes in UV-VIS spectra during photolysis of irradiated ENBO/CF_3CCl_3 solutions at 77 K (λ > 400 nm). (*b*) Difference UV-VIS spectra of the same solutions, normalized to the absorbance at their absorption maxima.

The EPR spectrum of the final product after photolysis of RC **2**, measured at 77 K, is shown in Figure 2(*d*) (curve *1*) and is a doublet signal with a splitting of ~3.1 mT. Raising the temperature to 130 K results in a better resolution due to averaging of the magnetic resonance parameters *via* an increase in mobility in the frozen matrix, while the measured splittings amounted to ~3.1 mT (1H) and ~1.0 mT (2H) [Figure 2(*e*), curve *1*]. Subsequent cooling to 77 K restored the original doublet structure of the spectrum. The fit of the experimental EPR spectra of the final photolysis product was satisfactory using the following optimized values of the hfc constants: a_1(1H) = 3.09 mT, a_2(1H) = 1.08 mT and a_3(1H) = 0.82 mT (ΔH_{pp} = 1.00 mT) for the spectrum recorded at 77 K [Figure 2(*d*), curve *2*] and a_1(1H) = 3.09 mT, a_2(1H) = 1.16 mT and a_3(1H) = 0.89 mT (ΔH_{pp} = 0.75 mT) for the spectrum recorded at 130 K [Figure 2(*e*), curve *2*].

Since deprotonation[6,7] reactions are the primary phototransformation pathways for the RCs of cyclopentene oxide and cyclohexene oxide, which were initially considered to be analogous to the ENBO RC, it was decided to primarily investigate the various distonic RCs and radicals that can be formed by the ENBO RCs under current conditions as final products of photolysis. Calculations of the hfc constants for these intermediates have shown that none of these structures can correspond to the EPR spectra observed experimentally [Figures 2(*d*),(*e*), curves *2*].

The similarity between the experimentally observed intermediate species, which can be seen in the EPR spectra during photolysis of RC **2**, and the RCs of alkyl-substituted cyclohexanes stabilized in Freons at 77 K, which are visible in their respective EPR spectra,[13,14] is of note. Next, one should take into account the redshift in the UV-VIS spectra: for example, the absorption maximum for the methylcyclohexane RC is observed at ~570 nm.[15] Also, such RCs can undergo photoelimination reactions, cleaving off H_2 and affording the corresponding cycloalkene RCs.[16] Considering all of the above, cycloalkene RC structures were proposed for the final photolysis product.

The results of quantum chemical (DFT) calculations of the magnetic resonance parameters in a series of probable cycloalkene products showed that the RC of 3-oxatricyclo[3.2.1.$0^{2,4}$]oct-5-ene (**3**) [Figure 1(*c*)] is represented by parameters that can be successfully used to fit the experimental EPR spectra: for example, the calculated values of the hfc constants for the H^1–H^3 nuclei were 1.12, 3.79 and 0.72 mT, respectively. Calculations of the Mulliken spin and charge populations demonstrated that the charge in RC **3** is predominantly localized on the oxygen atom (> 0.5), with the spin distributed between the C atom in the double bond and the C atom bound to H^3 (0.16 and 0.69, respectively). Therefore, the RC of 3-oxatricyclo[3.2.1.$0^{2,4}$]oct-5-ene can be considered as a distonic species that does not absorb a significant amount of light in the region $\lambda > 400$ nm. This is confirmed by the quantum chemical calculation of the probabilities of the main electronic transitions in this species, their positions in the UV-VIS spectra and the corresponding oscillator strengths.

Based on the data obtained, the mechanism of phototransformation in form **2** of the ENBO RC appears to be as follows. Upon absorption of light, the C–C bond is formed again in the oxirane ring, and the spin and charge are localized simultaneously on the cycloalkyl fragment of the RC. The resulting paramagnetic species is stable at 77 K. As usual for the cycloalkane RC,[16] it undergoes photoelimination of H_2, affording the 3-oxatricyclo[3.2.1.$0^{2,4}$]oct-5-ene RC.

Thus, for the investigated oxirane RCs, the formation of RCs upon radiolysis is associated either with the cleavage of the C–C bond or with a significant increase in the interatomic distance between the carbon atoms in the oxirane ring. Furthermore, a change in the nature of the substituent at the oxirane ring dramatically affects the phototransformation pathways of the corresponding RCs.

This work was supported by the Russian Foundation for Basic Research (project no. 19-03-00015) with the use of equipment purchased on behalf of the Development Program of Moscow State University. Calculations were performed using the resources of the Supercomputing Center of M. V. Lomonosov Moscow State University.[17]

References

1 V. I. Fel'dman and M. Ya. Mel'nikov, *High Energy Chem.*, 2000, **34**, 236 (*Khim. Vys. Energ.*, 2000, **34**, 279).
2 *Radical Ionic Systems. Properties in Condensed Phases*, eds. A. Lund and M. Shiotani, Kluwer Academic Publishers, Dordrecht, 1991.
3 T. Bally, *Chimia*, 2007, **61**, 645.
4 I. D. Sorokin, V. I. Feldman, O. L. Melnikova, V. I. Pergushov, D. A. Tyurin and M. Ya. Melnikov, *Mendeleev Commun.*, 2011, **21**, 153.
5 I. D. Sorokin, O. L. Melnikova, V. I. Pergushov, D. A. Tyurin, V. I. Feldman and M. Ya. Melnikov, *High Energy Chem.*, 2012, **46**, 183 (*Khim. Vys. Energ.*, 2012, **46**, 228).
6 I. D. Sorokin, O. I. Gromov, V. I. Pergushov, D. A. Pomogailo and M. Ya. Mel'nikov, *Mendeleev Commun.*, 2018, **28**, 618.
7 I. D. Sorokin, O. I. Gromov, V. I. Pergushov, D. A. Pomogailo and M. Ya. Melnikov, *Mendeleev Commun.*, 2020, **30**, 67.
8 F. Neese, *Wiley Interdiscip. Rev.: Comput. Mol. Sci.*, 2018, **8**, e1327.
9 S. Grimme, *J. Chem. Phys.*, 2006, **124**, 034108.
10 F. Weigend and R. Ahlrichs, *Phys. Chem. Chem. Phys*., 2005, **7**, 3297.
11 V. Barone, P. Cimino and E. Stendardo, *J. Chem. Theory Comput.*, 2008, **4**, 751.
12 S. Sinnecker, A. Rajendran, A. Klamt, M. Diedenhofen and F. Neese, *J. Phys. Chem. A*, 2006, **110**, 2235.
13 M. Shiotani, M. Lindgren and T. Ichikawa, *J. Am.. Chem. Soc.*, 1990, **112**, 967.
14 M. Lindgren, M. Matsumoto and M. Shiotani, *J. Chem. Soc., Perkin Trans. 2*, 1992, 1397.
15 Y. Katsumura, T. Azuma, M. A. Quadir, A. S. Domazou and R. E. Buehler, *J. Phys. Chem.*, 1995, **99**, 12814.
16 M. Tabata and A. Lund, *Chem. Phys.*, 1983, **75**, 379.
17 V. Sadovnichy, A. Tikhonravov, V. Voevodin and V. Opanasenko, in *Contemporary High Performance Computing: From Petascale toward Exascale*, ed. J. S. Vetter, CRC Press, Boca Raton, 2013, pp. 283–307.

Received: 9th December 2020; Com. 20/6390